DOI: 10.1002/adma.200800338

Efficient and Flexible ITO-Free Organic Solar Cells Using Highly Conductive Polymer Anodes**

By *Seok-In Na, Seok-Soon Kim, Jang Jo,* and *Dong-Yu Kim**

The introduction of donor-acceptor heterojunctions rendered small molecules and conjugated polymers attractive candidates for the fabrication of flexible cost-efficient power sources.[1] In particular, polymer bulk-heterojunction (BHJ) solar cells based on interpenetrating networks of electron-donor and -acceptor materials have undergone considerable development, including improvements in organic synthesis and fabrication methods.[2–10] Despite the relatively low efficiency in comparison with conventional inorganic solar cells, the potential of roll-to-roll processing and large-area processability on flexible low-cost substrates renders conjugated polymer-based organic solar cells (OSCs) very attractive as a cost-effective solution to the problem of energy shortage.

Among the available BHJ systems, poly(3-hexylthiophene) (P3HT) and 1-(3-methoxycarbonyl)-propyl-1-phenyl-(6,6)C_{61} (PCBM) networks produced by spin-coating have shown the highest efficiency – up to ~4–5% under 80 or 100 mW cm^{-2} illumination with air mass (AM) 1.5 global (G) conditions.[11–13] However, current state-of-the-art OSCs are typically fabricated on rigid glass substrates coated with indium tin oxide (ITO), and as a result do not make full use of the processing advantages of organic materials. Furthermore, even in the emergent generation of flexible devices, cells remain dependent on transparent conductive oxides such as ITO.[14,15] In fact, ITO is not an ideal conductive material, due to the following inherent problems: release of oxygen and indium into the organic layer, poor transparency in the blue region, and complete crystallization of ITO films, which requires high-temperature processing.[16] In particular, the ever-increasing cost of indium prevents large-scale use of ITO in low-cost photovoltaic energy conversion. Thus, it is clear that organic-based electrode materials should be intensively developed for use in both flexible- and rigid-substrate devices.

The most promising organic-based electrode material is poly(3,4-ethylenedioxythiophene):poly(styrenesulfonate) (PEDOT:PSS), which is extensively used as an interfacial layer to improve hole injection in most organic devices. Currently, various modifications of PEDOT:PSS with even greater conductivities are being investigated as electrodes for organic devices.[17–31] In particular, Zhang et al. and Ouyang et al. evaluated the possibility of substituting ITO by using PEDOT:PSS with sobitol and meso-erythritol, respectively, as anodes in OSCs based on poly(2-methoxy-5-(2′-ethylhexyloxy)-1,4-phenylene vinylene) (MEH-PPV) and PCBM.[17,20] In addition, to further enhance conductivity of a pure-PEDOT anode in a polymer solar cell, Aernouts et al. applied a metallic Ag grid to PEDOT:PSS, and Glatthaar et al. reported an inverted cell by using a PEDOT anode with thermally deposited Au lines.[29,30] Most recent, Tvingstedt et al. demonstrated the possibility of substituting the ITO in organic photovoltaic cells using an anode comprising PEDOT and metallic micro-Ag-grids, which were formed using a soft-lithography metal-deposition method.[31] Although most of the above-mentioned studies have successfully demonstrated the possibility of substituting the ITO with PEDOT or PEDOT with a metal grid in OSCs, the OSC power-conversion efficiencies remained low – less than 1.5% – compared with those of current state-of-the-art OSCs (~4–5%). Thus, further efforts should be devoted to the production of ITO-free OSCs with high efficiency – comparable to those of ITO-based OSCs – on flexible and rigid substrates alike, for low-cost power generation.

The aim of this work is to fabricate an ITO-free organic solar cell with high efficiency and good flexibility, using an organic-based electrode material to completely replace ITO. We investigated a recently developed PEDOT:PSS formulation, Baytron PH 500, provided by H. C. Starck, as a polymer anode in plastic solar cells, which recently showed the possibility of use as the anode in a small-molecule-based organic light-emitting diode (OLED).[32] Here, we describe ITO-free OSCs fabricated on glass and flexible plastic substrates. The efficiency of the these cells (3.27% and 2.8%, respectively, under 100 mW cm^{-2} illumination with AM 1.5 G condition) was comparable to that of ITO-based devices fabricated on glass and on flexible substrates (3.66% and 2.9%,

[*] Prof. D.-Y. Kim, S.-I. Na, J. Jo
Heeger Center for Advanced Materials
Department of Materials Science and Engineering
Gwangju Institute of Science and Technology
1 Oryong-Dong, Buk-Gu, Gwangju 500-712 (Korea)
E-mail: kimdy@gist.ac.kr
Prof. S.-S. Kim
School of Materials Science and Chemical Engineering
Kunsan National University
Kunsan, Chonbuk, 573-701(Korea)

[**] We thank Dr. A. Sautter and Dr. A. Elschner from H.C. Starck for their stimulating discussions and for providing PEDOT:PSS (PH 500). This work was financially supported by the Heeger Center for Advanced Materials (HCAM), the Ministry of Education of Korea through Brain Korea 21 (BK21) program, and the Korea Science and Engineering Foundation (KOSEF) through the National Research Lab Program funded by the Korean government (MEST, M10500 000077-06J0000-07710). Supporting Information is available online from Wiley InterScience or from the authors.

© 2008 WILEY-VCH Verlag GmbH & Co. KGaA, Weinheim

ADVANCED MATERIALS

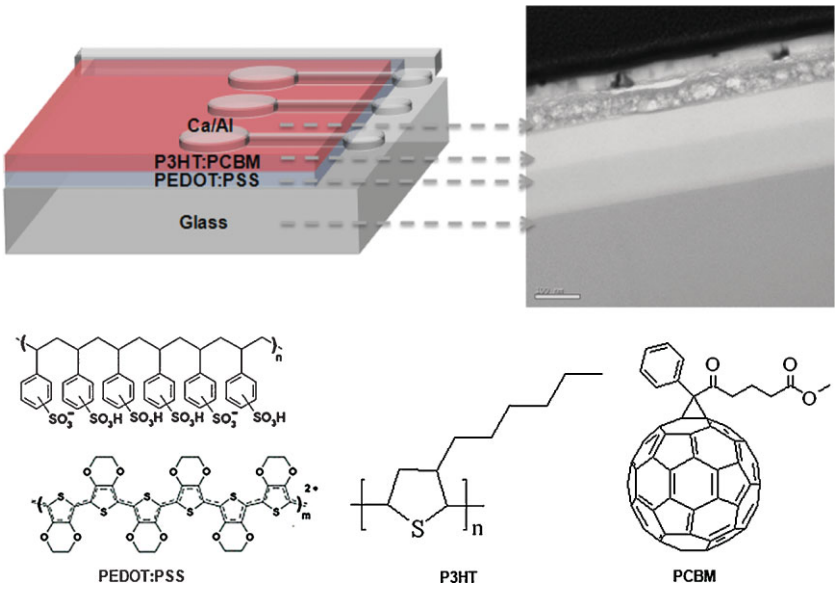

Figure 1. Device structure and TEM cross-sectional image (scale bar: 100 nm) of the polymer solar cell with a PEDOT anode (upper part) and molecular structures of PEDOT:PSS, P3HT, and PCBM, used in the cell (lower part).

respectively) under equivalent conditions. Furthermore, while ITO-based cells on flexible substrates showed a power conversion efficiency of 0% after 75 bending cycles during the flexibility test, the efficiency of ITO-free OSCs with PEDOT anodes (power conversion efficiency of 2.73%) remained unchanged after more than 300 bending cycles, demonstrating superior mechanical robustness compared to ITO-based cells.

Figure 1 shows the structure of the ITO-free OSC (IFOSC) with a PEDOT:PSS anode; the chemical structure of its components is also shown. The highly conductive polymer-anode first layer was prepared by addition of 5% dimethylsulfoxide (DMSO) to PH 500 (hereafter, referred to as modified PH500 or PEDOT anode). The modified PH500 was spin-coated at 2000 rpm for 10 seconds and then annealed at ~120 °C for 20 min, producing a film 100 nm thick. The second layer is a bulk-heterojunction composite of P3HT and PCBM that forms an active layer ~80 nm thick. Finally, calcium and aluminum were thermally evaporated to form the cathode. A cross-sectional high-resolution transmission electron microscopy (TEM) image of the prepared polymer solar cell (Fig. 1) clearly shows the individual layers and a distinct interface; there is no interlayer mixing. More importantly, there is no ITO layer, which typically appears darker than the glass and PEDOT:PSS layer in TEM images of ITO-based OSCs.[33]

Conductivity was evaluated using four-point-probe measurements obtained for a series of PEDOT:PSS and ITO films on glass and polyethyleneterephthalate (PET) substrates, respectively, as shown in Figure 2. The preparation of PEDOT:PSS films is described in the Experimental section. The conductivity of each PEDOT:PSS and ITO film was plotted as the average of measurements taken at the center and edges of three glass samples and three PET samples, and the conductivities of the PEDOT:PSS films on the glass and plastic substrates were similar. As shown in Figure 2, pure PH500 ($<1\,S\,cm^{-1}$) had a relatively high conductivity compared with VPAI 4083 ($<\sim10^{-3}\,S\,cm^{-1}$), which is normally used as an interfacial layer for better hole-injection in optoelectronic devices. In particular, modified PH500 recorded a peak conductivity of $\sim550\,S\,cm^{-1}$ and an average conductivity of $\sim470\,S\,cm^{-1}$, while ITO-coated PET (Aldrich Co, Ltd., 40 Ω/square) and ITO-coated glass (Samsung Corning Co, Ltd., 10 Ω/square) had average conductivities of ca. $1050\,S\,cm^{-1}$ and ca. $6740\,S\,cm^{-1}$, respectively. Thus, the conductivity of modified PH500 was twofold lower and one order of magnitude lower than those of ITO/PET and ITO/Glass, respectively. The conductivity enhancement of PEDOT:PSS films by adding a polar solvent with a high boiling point, such as DMSO, N-methylpyrrolidone (NMP), *N*,*N*-dimethylformamide (DMF), and ethylene glycol (EG), has been widely studied and discussed.[19–23] For a better examination, we investigated the effects of each solvent on the conductivity enhancement of PEDOT:PSS films (Fig. SI-1). The conductivity of PH500 was significantly increased by the addition of DMF, EG, and NMP, and the DMSO-added PH500 sample showed maximum conductivity. In addition, the conductivities of modified PH500 increased with added DMSO concentration, and tended toward a saturation value (Fig. SI-2). Although conductivities showed similar values for concentrations higher than 5% DMSO, the achievement of smooth surface morphologies, which is another important factor affecting the efficiency of organic-based devices, was difficult. Considering

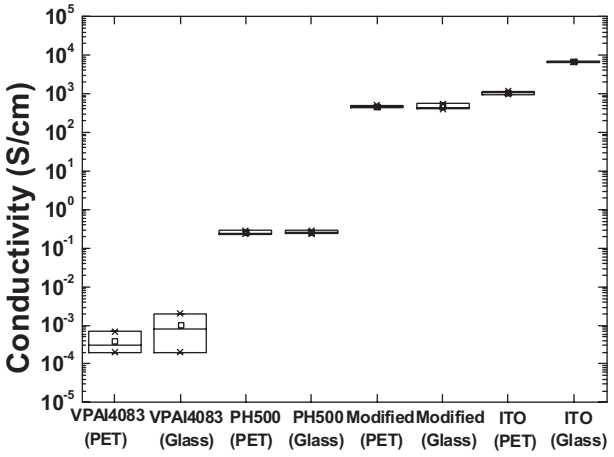

Figure 2. Conductivities of VPAI4083, PH500, modified PH500, and ITO, on glass and on plastic substrates.

© 2008 WILEY-VCH Verlag GmbH & Co. KGaA, Weinheim

both conductivity and film uniformity, addition of 5% DMSO is considered to be an optimal condition for transparent electrodes in organic-based devices.

The morphology of modified PH500 was investigated to determine why conductivity was enhanced by adding 5% DMSO, since it is believed that distribution of PEDOT:PSS gel-particles determines the physical properties of the thin film. The size of the PEDOT:PSS particles was increased by adding 5% DMSO, compared to that of films prepared with pure PH500 (Fig. SI-3). Here, the particle size can be definitively linked to film conductivity, because as the particles grow the total number of particle boundaries in a given volume or area can decrease. Therefore, conductivity enhancement might be attributed to an increased particle size due to decreased particle boundaries, namely, fewer energy barriers. Although the mechanism of enhancing conductivity of PEDOT:PSS films by addition of polar solvents has been intensively investigated,[18–25] some controversy may remain concerning the fundamental principle involved. For example, Huang et al.[18] suggested that the improvements in conductivity are attributed to morphology changes that lead to larger grain sizes and lower intergrain hopping. Kim et al.[19] reported that the conductivity can be increased mainly due to the screening effects of the polar solvents. Jönsson et al.[23] proposed that excess PSS is washed away from the surface of the PEDOT:PSS grains in the film, creating a better connection between the conducting PEDOT:PSS grains. Pettersson et al.[24] reported that the polyalcohol induces a reorientation of the PEDOT:PSS chains, leading to better connections between the conducting PEDOT chains. Therefore, we believed that further efforts were needed in order to more clearly explain the origins of this conductivity enhancement.

To directly investigate modified PH500 as an anode for IFOSCs and the effects of conductivity on IFOSC performance, we fabricated several identical OSCs that varied only in their respective anode. The tested anodes were as follows: VPAI4083, PH500, modified PH500 (see Fig. 1), and ITO/Glass underneath VPAI 4083, which was used as a reference anode for conventional OSCs. Representative results from each device are presented in Figure 3. Photocurrent density–voltage (*J–V*) curves were obtained under 100 mW cm^{-2} illumination with AM 1.5 G conditions, as shown in Figure 3a. The device with the modified PH500 anode exhibited excellent performance characteristics, as follows: short-circuit current (J_{sc}) of 9.73 mA cm^{-2}, open-circuit voltage (V_{oc}) of ~0.63 V, fill-factor (FF) of 53.5%, and power conversion efficiency (η_p) of 3.27%. In contrast, the performance of devices with VPAI4083 and pure PH500 anodes was very poor, as shown in the inset of Figure 3a. This result is believed to come from the significantly lower series resistance in the IFOSC with modified-PH500 anodes, and is confirmed by much higher FF and photocurrent for the IFOSC with modified-PH500 anode compared with the other PEDOT anodes, as summarized in Table 1. It is worth noting that the photovoltaic characteristics of the IFOSC with modified-PH500 anode were, as shown in Table 1, comparable to those of conventional ITO-based OSCs.

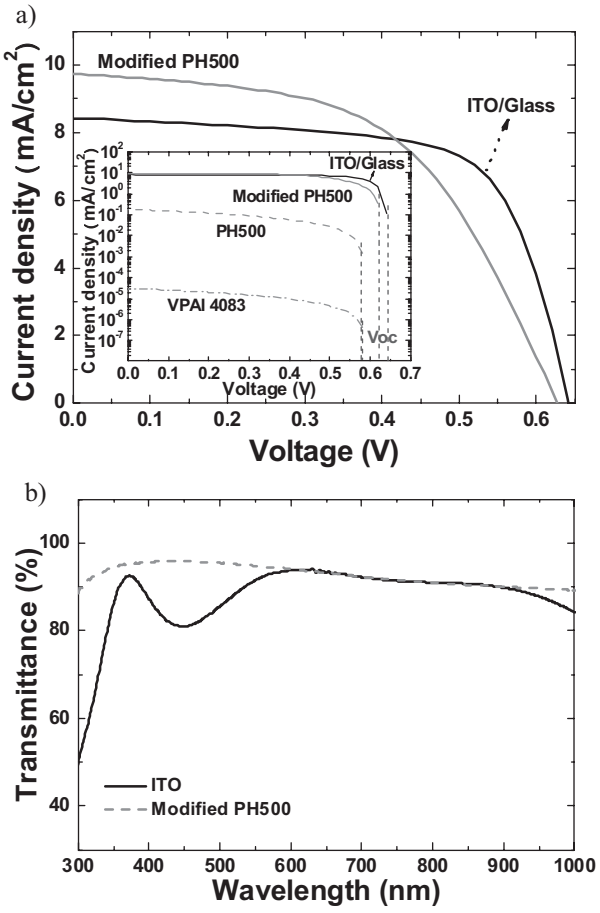

Figure 3. a) *J–V* characteristics for two kinds of solar cells: an ITO-free cell with a modified PH500 anode and a conventional cell with ITO/Glass underneath VPAI4083 as a reference anode. Inset: *J–V* characteristics for solar cells constructed with four different anodes. b) Transmission spectra of modified PH500 and ITO, excluding individual glass substrates.

Materials that are used for anodes in photovoltaic cells require high transparency as well as high conductivity. Optical transmission spectra of the representative anodes used in this study are shown in Figure 3b. Compared with modified PH500, the optical transmittance of ITO excluding the glass substrate is much lower in the wavelength range 300–600 nm. The optical transmission of the modified PH500 excluding the glass substrate is quite flat and more than 90% across most of the full visible range. Thus, the increase in photocurrent of IFOSCs

Table 1. Photovoltaic parameters and efficiencies of ITO-free OSCs with different PEDOT:PSSs as anodes and conventional ITO-based OSC.

	J_{sc}(mA cm^{-2})	FF (%)	V_{oc} (V)	η_p (%)
VPAI 4083	3×10^{-5}	25.0	0.577	4×10^{-6}
PH500	0.184	25.3	0.579	0.03
Modified PH500	9.73	53.5	0.627	3.27
ITO/Glass	8.42	67.8	0.641	3.66

© 2008 WILEY-VCH Verlag GmbH & Co. KGaA, Weinheim

ADVANCED MATERIALS

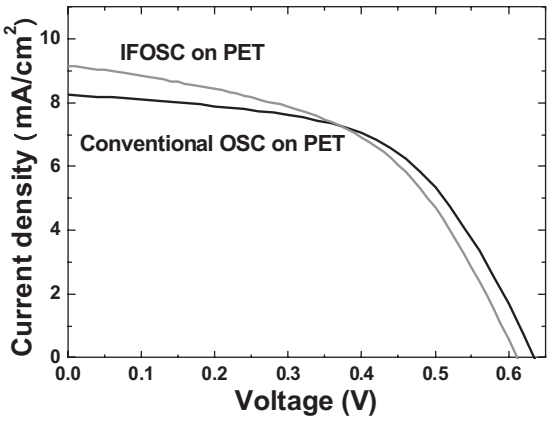

Figure 4. *J–V* characteristics of two solar cells on flexible substrates: an ITO-free cell with a PEDOT anode and a conventional cell with ITO/PET underneath VPAI4083 as a reference anode.

with modified PH500 (see Fig. 3a and Table 1) compared to that of ITO-based cells likely results from enhanced transmittance in the main absorption region (300–600 nm) of P3HT/PCBM-based OSCs.

In recent years, interest in flexible optoelectronic devices has increased due to advantages such as portability and malleability. For instance, one possible application is covering nonflat surfaces such as roofing tiles, walls, and fences with flexible plastic solar cells – task that would be difficult with a rigid material. In this respect, we investigated potential uses of modified PH500 as an electrode in flexible devices. Modified PH500 was used as the anode, and ITO/PET underneath VPAI4083 was used as a reference anode in conventional flexible OSCs. A sandwiched structure of solar cells on PET substrates identical to that of cells on rigid glass substrates was used. After separate spin-coating processes were performed, the films were annealed. The PEDOT films and the active films on PET were annealed at 100 °C for 20 min and 10 min, respectively, due to significant thermal shrinkage of plastic PET substrates during high-temperature processes.[34] Performance characteristics of the two cells, obtained under 100 mW cm^{-2} illumination and AM 1.5 G conditions, are shown in Figure 4. The IFOSC with the PEDOT anode exhibited superior performance even on plastic substrates, as follows: $J_{sc} = 9.16\,mA\,cm^{-2}$, $V_{oc} = 0.61\,V$, FF = 50%, and $\eta_p = 2.8\%$. The performance characteristics of IFOSC on PET were comparable to those of IFOSC on glass, because the conductivities of modified PH500 anodes on glass and PET substrates were comparable, as shown in Figure 2. In addition, the performance of the IFOSC on PET was nearly identical to that obtained for ITO-based OSC on PET ($J_{sc} = 8.24\,mA\,cm^{-2}$, $V_{oc} = 0.63\,V$, FF = 56%, and $\eta_p = 2.9\%$). The primary difference between the device with ITO on PET and that constructed with ITO on glass is in FF. Use of PET, rather than glass, as the substrate for ITO reduced FF from 67.8% to 56%, suggesting that most of the decrease in cell efficiency is due to a reduction in FF rather than V_{oc} and J_{sc}. The decrease in FF reflects the higher series resistance in the cell with ITO on PET, and this observation is in agreement with the conductivities of ITO/PET and ITO/Glass, as shown in Figure 2. These results are attributed to the low-temperature process required for deposition of ITO on plastic substrates, that can produce porous films with lower conductivity, reduced transparency, and poor adhesion, leading to reduced device performance.[27,35]

To further explore the feasibility of flexible devices, we analyzed the mechanical stability of IFOSC and conventional OSC on PET. Representative results of these flexible devices are presented in Figure 5. The performance of conventional OSCs on PET during repeated bending cycles at a radius of ~8 mm declined dramatically, as shown in Figure 5a. In particular, after five bending cycles the efficiency of cell decreased by as much as ~40%. In contrast, the performance of

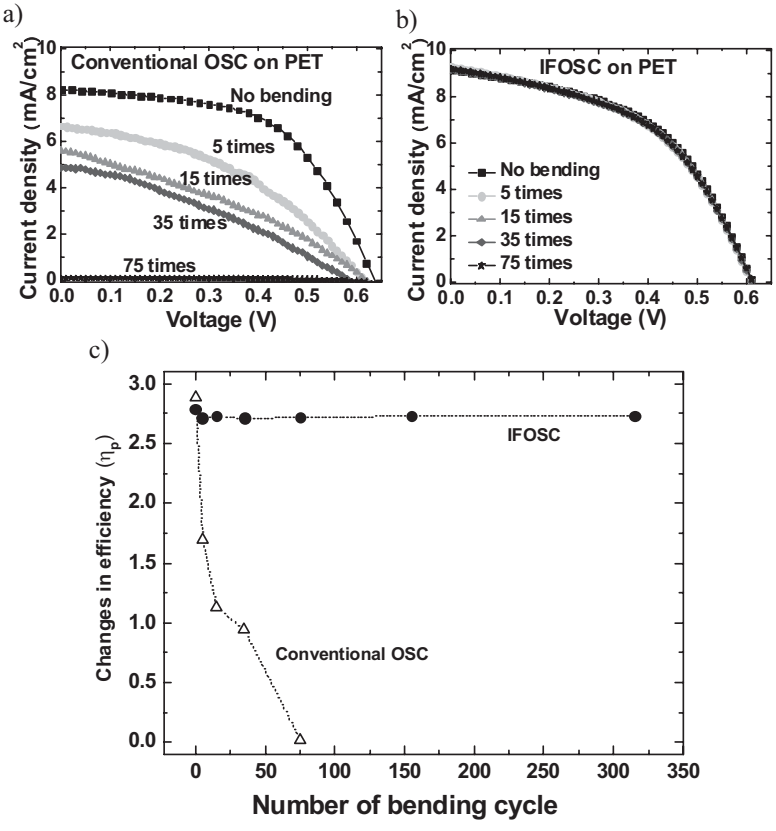

Figure 5. Changes in *J–V* characteristics for two solar cells on flexible PET substrates during repeated bending: a) a conventional ITO-based OSC and b) a IFOSC with a PEDOT anode. c) Changes in efficiency of a conventional ITO-based OSC and an IFOSC with a PEDOT anode during repeated bending.

 © 2008 WILEY-VCH Verlag GmbH & Co. KGaA, Weinheim

IFOSCs constructed with PEDOT remained nearly constant during the flexibility test, as demonstrated in Figure 5b. Furthermore, after only 75 bending cycles, the η_p of the ITO-based cell was almost 0%, as shown in Figure 5c, while the efficiency of the flexible IFOSC with PEDOT anode, in contrast, remained nearly constant ($\eta_p = 2.73\%$), even after more than 300 bending cycles.

To obtain detailed information about the failure of ITO-based cells during the flexibility test, the sequence of layers were investigated, as shown in Figure 6. First, the brittle nature of the ITO anode was investigated and compared to the PEDOT anode. The behavior of both ITO and PEDOT layers during repeated bending is plotted in Figure 6a. While the resistance of PEDOT remained relatively constant, ITO degraded rather quickly, showing a ~40-fold increase in resistance after ~2500 bending cycles at a radius of ~8 mm, compared with the initial resistance. The dramatic increase in resistance in the ITO anode was attributed to the formation and propagation of cracks, as shown in the upper inset of Figure 6a.[36] In contrast, there was no evidence of crack formation in the PEDOT anode after ~2500 bending cycles, as shown in the lower inset of Figure 6a. More importantly, crack formation and propagation were evident in the active layers (see Fig. 6b) and metal cathodes (see Fig. 6c) of conventional ITO-based cells after only 100 bending cycles. However, the active layer and metal cathode of an IFOSC with the PEDOT anode had clean surfaces that were free of cracks after more than 300 bending cycles, as shown in Figures 6d and e. In addition, the surface profile of metal cathodes (see the inset of Fig. 6c) of conventional ITO-based cells showed very irregular and rough surfaces on the micrometer scale due to the generated cracks, compared with the smooth surface of metal cathodes of IFOSC (see the inset of Fig. 6e). Consequently, failure of the ITO-based cell during the initial stage of the flexibility test can be attributed to the formation of severe cracks throughout the sequence of layers (i.e., ITO anode, active layer, and metal cathode), significantly limiting efficient charge separation and transport. From this point of view, the polymer anode is better suited than the ITO anode for fabrication of flexible low-cost photovoltaic cells.

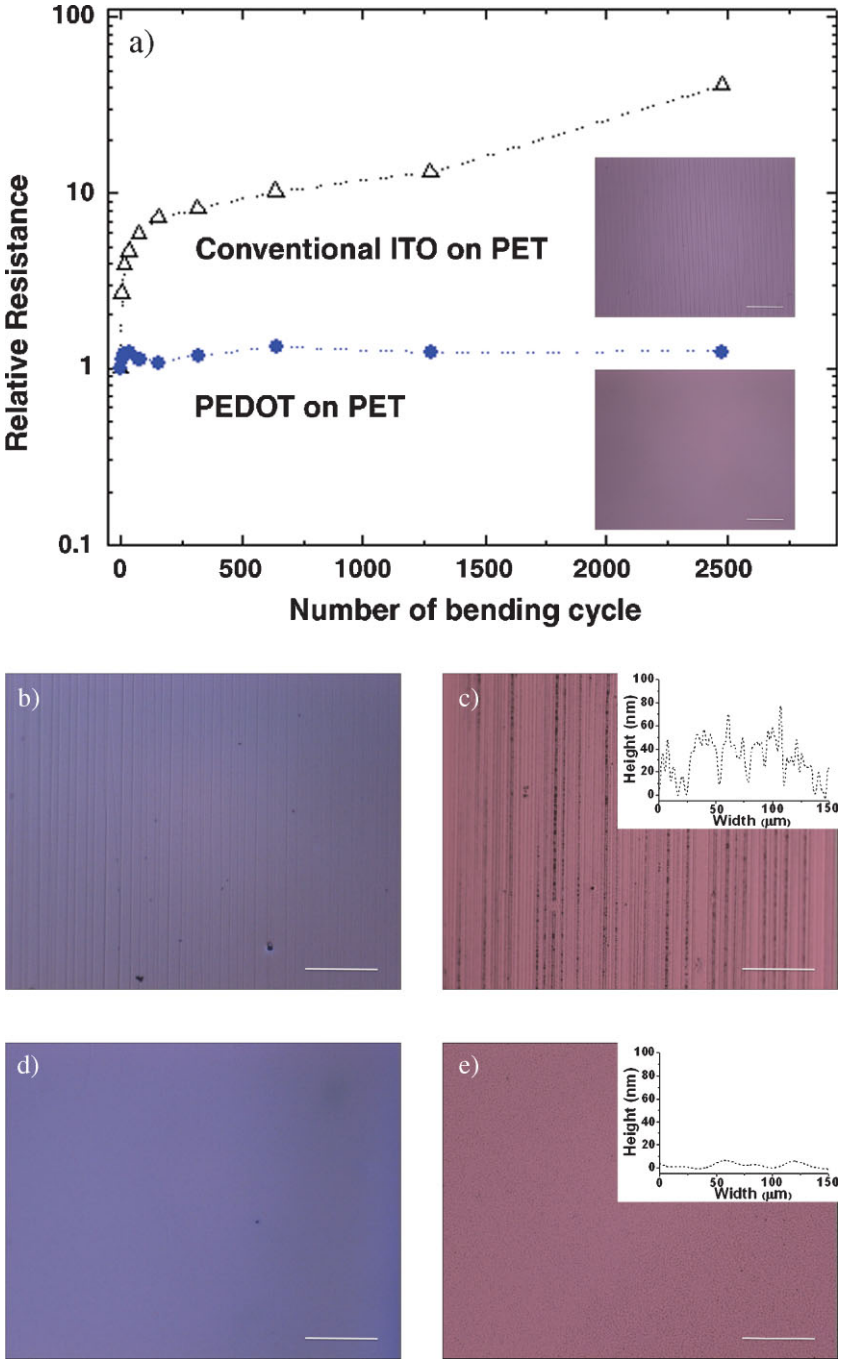

Figure 6. a) Relative resistance of ITO and PEDOT on flexible PET substrates during repeated bending (insets: optical microscopy images of ITO and PEDOT films after the bending test) and optical microscopy images of b) an active layer in a conventional ITO-based OSC, c) a metal cathode in a conventional ITO-based OSC, d) an active layer in IFOSC with a PEDOT anode, and e) a metal cathode in IFOSC with a PEDOT anode (scale bars: 100 μm) (insets of (c) and (e): surface profiles of the metal cathodes in a conventional ITO-based OSC and in a IFOSC after the bending test.)

In conclusion, highly efficient ITO-free OSCs with conductive polymer anodes (highly conductive PH500 doped with 5% DMSO) on both glass and flexible plastic substrates were demonstrated for the first time. The efficiencies of ITO-free OSCs on glass and flexible plastic substrates (3.27% and 2.8%, respectively, under 100 mW cm^{-2} with AM 1.5 G) were

© 2008 WILEY-VCH Verlag GmbH & Co. KGaA, Weinheim

ADVANCED MATERIALS

comparable to those of ITO-based devices on glass and flexible substrates (3.66% and 2.9%, respectively, under equivalent conditions), which are thought to be the highest reported to date. Furthermore, in the flexibility test, the ITO-free OSCs with PEDOT anodes on the flexible substrate manifested superior mechanical robustness compared with ITO-based cells. All ITO-free OSC characteristics clearly demonstrate that the highly conductive polymeric material shows potential as a practical replacement for expensive and brittle ITO. The high efficiency and good flexibility of ITO-free OSCs will advance the production of flexible low-cost OSCs by high-throughput roll-to-roll manufacturing.

Experimental

ITO-coated glass (Samsung Corning Co, Ltd., 10 Ω/square) and ITO-coated PET (Aldrich Co, Ltd., 40 Ω/square) substrates were used for rigid and flexible ITO-based devices, respectively. To ensure use of identical substrates for the rigid and flexible ITO-free OSCs, all ITO on the ITO-coated glass and ITO-coated PET substrates was etched using an ITO wet-etching solution of $HCl/HNO_3/H_2O$. For cell fabrication and measurement of conductivity, glass, PET, ITO-coated glass, and ITO-coated PET substrates were cleaned with a special detergent followed by ultrasonication in acetone and isopropyl alcohol, and then were kept at 100 °C for ~30 min. All substrates were treated with UV/ozone to improve the wettability of PEDOT:PSS.

Film conductivities were measured using a standard four-point-probe system with a Keithley 2400 current source and an HP 34420A nanovoltmeter. VPAI4083, which was used as a standard PEDOT:PSS (Baytron P VPAI 4083, purchased from H. C. Starck), PH500 (Baytron PH 500, provided by H. C. Starck), and modified PH500 were spin-coated at 2000 rpm for 10 s. PEDOT:PSS films on glass and PET were annealed at 120 °C and 100 °C, respectively, for 20 min.

Modified PH500 was spin-coated using an aqueous solution that had been filtered using a 0.45-μm filter, and was subsequently annealed at 120 °C for 20 min. The cell constructed with the PET substrate was annealed at 100 °C for 20 min in air. Conventional ITO-based OSCs were constructed as follows. Standard PEDOT:PSS (Baytron P VPAI 4083) was spin-coated onto glass and PET and then annealed under the same conditions used for ITO-free OSCs, producing films ~20 nm thick.

For the fabrication of photoactive layers composed of interconnected networks of electron-donors and acceptors, P3HT (Rieke Metals) and PCBM (Nano-C) were dissolved in chlorobenzene to make 30 mg mL^{-1} and 15 mg mL^{-1} solutions, respectively, followed by shaking at room temperature for ~12 h. The P3HT–PCBM blend was then prepared by mixing the two separate solutions. A homogeneously mixed blend system was obtained by shaking the mixture for ~12 h. ITO-free OSCs and conventional ITO-based OSCs on glass substrates were fabricated by spin-coating the blend solution at room temperature and subsequently annealing at 110 °C for 10 min. The PET devices were annealed at 100 °C for 10 min in N_2. Fabrication of the devices was completed by thermal evaporation of a Ca/Al (20 nm/80 nm) metal top electrode with an area of 4.34 mm^2 in vacuum with a pressure of 10^{-6} Torr (1.33×10^{-4} Pa).

Cell performance was measured under 1-sun using a xenon light source and an AM 1.5 global filter under nitrogen atmosphere without encapsulation. Photocurrent-voltage (*I–V*) measurements were performed using a Keithley 4200 instrument. A calibrated silicon reference solar cell certified by the National Renewable Energy Laboratory (NREL) was used to confirm the measurement conditions of our set-up. The flexibility of ITO-free OSCs and conventional ITO-based cells was investigated using an in-house bending-test system sized to fit in a glove box. During the bending test, changes in cell performance were measured using a Keithley 4200 instrument in N_2, and the resistances of PEDOT and ITO anodes were measured using a Keithley 2400 current source and an HP 34420A nanovoltmeter in air.

The thickness of all films was measured using a surface profiler (Kosaka ET-3000i). The UV-vis transmission spectra were measured using a Perkin-Elmer Lambda 12 UV/Vis spectrophotometer. Cross-sectional TEM images were obtained using a field-emission TEM (FEI Tecnai F30 S-Twin) operated at 300 kV. TEM samples were prepared using a focused ion beam (FIB, NOVA200) to vertically cut the entire ITO-free P3HT:PCBM solar cell with a buffer layer of Pt deposited on the top surface.

Received: February 2, 2008
Revised: May 2, 2008
Published online:

[1] C. W. Tang, *Appl. Phys. Lett.* **1986**, *48*, 183.
[2] N. S. Sariciftci, L. Smilowitz, A. J. Heeger, F. Wudl, *Science* **1992**, *258*, 1474.
[3] G. Yu, J. Gao, J. C. Hummelen, F. Wudl, A. J. Heeger, *Science* **1995**, *270*, 1789.
[4] C. J. Brabec, N. S. Sariciftci, J. C. Hummelen, *Adv. Funct. Mater.* **2001**, *11*, 15.
[5] X. Yang, J. Loos, S. C. Veenstra, W. J. H. Verhees, M. M. Wienk, J. M. Kroon, M. A. J. Michels, R. A. J. Janssen, *Nano Lett.* **2005**, *5*, 579.
[6] F. C. Krebs, H. Spanggaard, *Chem. Mater.* **2005**, *17*, 5235.
[7] S.-S. Kim, S.-I. Na, J. Jo, G. Tae, D.-Y. Kim, *Adv. Mater.* **2007**, *19*, 4410.
[8] A. Cravino, P. Schilinsky, C. J. Brabec, *Adv. Funct. Mater.* **2007**, *17*, 3906.
[9] D. Vak, S.-S. Kim, J. Jo, O.-S. Oh, S.-I. Na, J. Kim, D.-Y. Kim, *Appl. Phys. Lett.* **2007**, *91*, 081102.
[10] M.-S. Kim, J.-S. Kim, J. C. Cho, M. Shtein, L. J. Guo, J. Kim, *Appl. Phys. Lett.* **2007**, *90*, 123113.
[11] W. Ma, C. Yang, X. Gong, K. Lee, A. J. Heeger, *Adv. Funct. Mater.* **2005**, *15*, 1617.
[12] S.-I. Na, S.-S. Kim, S.-S. Kwon, J. Jo, J. Kim, T. Lee, D.-Y. Kim, *Appl. Phys. Lett.* **2007**, *91*, 173509.
[13] G. Li, V. Shrotriya, J. Huang, Y. Yao, T. Moriarty, K. Emery, Y. Yang, *Nat. Mater.* **2005**, *4*, 864.
[14] H. Han, D. Adams, J. W. Mayer, T. L. Alford, *J. Appl. Phys.* **2005**, *98*, 083705.
[15] J. Lewis, S. Grego, B. Chalamala, E. Vick, D. Temple, *Appl. Phys. Lett.* **2004**, *85*, 3450.
[16] J. Cui, A. Wang, N. L. Edleman, J. Ni, P. Lee, N. R. Armstrong, T. J. Marks, *Adv. Mater.* **2001**, *13*, 1476.
[17] F. Zhang, M. Johansson, M. R. Andersson, J. C. Hummelen, O. Inganäs, *Adv. Mater.* **2002**, *14*, 662.
[18] J. Huang, P. F. Miller, J. S. Wilson, A. J. de Mello, J. C. de Mello, D. D. C. Bradley, *Adv. Funct. Mater.* **2005**, *15*, 290.
[19] J. Y. Kim, J. H. Jung, D. E. Lee, J. Joo, *Synth. Met.* **2002**, *126*, 311.
[20] J. Ouyang, C.-W. Chu, F.-C. Chen, Q. Xu, Y. Yang, *Adv. Funct. Mater.* **2005**, *15*, 203.
[21] J. Ouyang, Q. Xu, C.-W. Chu, Y. Yang, G. Li, J. Shinar, *Polymer* **2004**, *45*, 8443.
[22] Baytron homepage. http//:www.baytron.com (accessed: December, 2007).
[23] S. K. M. Jönsson, J. Birgerson, X. Crispin, G. Greczynski, W. Osikowicz, A. W. Denier van der Gon, W. R. Salaneck, M. Fahlman, *Synth. Met.* **2003**, *139*, 1.

 © 2008 WILEY-VCH Verlag GmbH & Co. KGaA, Weinheim

[24] L. A. A. Pettersson, S. Ghosh, O. Inganäs, *Org. Electron.* **2002**, *3*, 143.
[25] X. Crispin, F. L. E. Jakobsson, A. Crispin, P. C. M. Grim, P. Andersson, A. Volodin, C. van Haesendonck, M. van der Auweraer, W. R. Salaneck, M. Berggren, *Chem. Mater.* **2006**, *18*, 4354.
[26] P. A. Levermore, L. Chen, X. Wang, R. Das, D. D. C. Bradley, *Adv. Mater.* **2007**, *19*, 2379.
[27] J. Huang, X. Wang, Y. Kim, A. J. de Mello, D. D. C. Bradley, J. C. de Mello, *Phys. Chem. Chem. Phys.* **2006**, *8*, 3904.
[28] S. Admassie, F. Zhang, A. G. Manoj, M. Svensson, M. R. Andersson, O. Inganäs, *Sol. Energy Mater. Sol. Cells* **2006**, *90*, 133.
[29] T. Aernouts, P. Vanlaeke, W. Geens, J. Poortmans, P. Heremans, S. Borghs, R. Mertens, R. Andriessen, L. Leenders, *Thin Solid Films* **2004**, 451–52, 22.
[30] M. Glatthaar, M. Niggemann, B. Zimmermann, P. Lewer, M. Riede, A. Hinsch, J. Luther, *Thin Solid Films* **2005**, *491*, 298.
[31] K. Tvingstedt, O. Inganäs, *Adv. Mater.* **2007**, *19*, 2893.
[32] K. Fehse, K. Walzer, K. Leo, W. Lövenich, A. Elschner, *Adv. Mater.* **2007**, *19*, 441.
[33] J. Y. Kim, K. Lee, N. E. Coates, D. Moses, T.-Q. Nguyen, M. Dante, A. J. Heeger, *Science* **2007**, *317*, 222.
[34] R. D. Deanin, *Polymer Structure, Properties and Applications*, Cahners Books, Boston **1972**.
[35] S. Ray, R. Banerjee, N. Basu, A. K. Batabyal, A. K. Barua, *J. Appl. Phys.* **1983**, *54*, 3497.
[36] Z. Chen, B. Cotterell, W. Wang, E. Guenther, S.-J. Chua, *Thin Solid Films* **2001**, *394*, 202.

 © 2008 WILEY-VCH Verlag GmbH & Co. KGaA, Weinheim